Available online at www.sciencedirect.com
ScienceDirect
Digital Signal Processing 16 (2006) 682–694
Digital Signal Processing
www.elsevier.com/locate/dsp

On the application of cross correlation function to subsample discrete time delay estimation ☆

Lei Zhang *, Xiaolin Wu

Department of Electrical and Computer Engineering, McMaster University, Hamilton, Ontario, Canada, L8S 4K1

Available online 15 September 2006

Abstract

Cross correlation function (CCF) of signals is an important tool of multi-sensors signal processing. Parabola functions are commonly used as parametric models of the CCF in time delay estimation. The parameters are determined by fitting samples near the maximum of the CCF to a parabola function. In this paper we analyze the CCF for the stationary processes of exponential auto-correlation function, with respect to two important types of sensor sampling kernels. Our analysis explains why the parabola is an acceptable model of CCF in estimating the time delay. More importantly, we demonstrate that the Gaussian function is a better and more robust approximation of CCF than the parabola. This new approximation approach leads to higher precision in time delay estimation using the CCF peak locating strategy. Simulations are also carried out to evaluate the performance of the proposed estimation method for different sample window sizes and signal to noise ratios. The new method offers significant improvement over the current parabola based method.

Keywords: Time delay estimation; Cross correlation; Parametric model

1. Introduction

Multiple sensors are widely used for robust estimation, communication and target tracking. When several sensors of different physical characteristics and varying spatial locations sample a continuous time signal, they produce correlated time sequences. The cross correlation between any two of the sampled signals contains vital information about the original signal, and can play an important role in applications such as multi-sensor data fusion and tracking [1,2], and sonar [3]. The cross correlation function (CCF) is a powerful tool for time delay estimation that registers different signals sampled by different sensors in time domain. An accurate time registration is crucial in processing of multi-sensor signals such as sonar [3], seismic data processing and tracking [4]. Similar problem arises in superresolution signal reconstruction, a process of creating a higher resolution representation of a signal from multiple lower resolution observations [5].

Time delay estimation of two analog signals through cross-correlation has been studied by many authors [6–13]. Knapp and Carter gave a maximum likelihood estimator of the relative delay between two continuous signals [6].

☆ This research is supported partially by Natural Sciences and Engineering Research Council of Canada.
* Corresponding author. Present address: Department of Computing, The Hong Kong Polytechnic University, Hung Hom, Kowloon, Hong Kong.
E-mail address: cslzhang@comp.polyu.edu.hk (L. Zhang).

1051-2004/$ – see front matter
doi:10.1016/j.dsp.2006.08.009

Azaria and Hertz [7] further reexamined this method for stationary signals. However, this method needs to know the spectra of signals and noise, and it applies to analog signals only. For digital systems a popular approach of time delay estimation is to locate the peak of CCF of the two discrete signals. The amount of delay is generally not an integral multiple of the sampling period. To estimate the delay in arbitrary precision, a common technique is to fit the CCF by a parabola with three samples in the neighborhood of the peak correlation value [9–11]. As alternatives to CCF, some methods use the average square difference function (ASDS) and the average magnitude difference function (AMDF) to estimate the time delay [9,11]. Other time delay estimation techniques exploit the high-order statistics of the data [14], or employ wavelet transform to whiten the data [13], or determine the time delay through a parameter optimization procedure in frequency domain [15].

In this paper we are interested in the analysis of CCF and the estimation of the time delay by locating the CCF's peak position with a small number of observed points of the CCF. We will derive the analytical forms of CCFs for Gaussian and box sensor kernels and for the class of stationary signals that have an exponentially decaying auto-correlation function (ACF). Our analysis explains why the parabola function can fit the CCF reasonably well, as previously believed in the literatures. More importantly, we establish Gaussian function to be a better and more robust approximation of CCF than the parabola function for all signals in the class considered above. Indeed, the new Gaussian model leads to superior performance in time delay estimation to the parabola-based method.

This paper is organized as follows. Section 2 introduces the discrete signal generation system and the problem of time delay estimation. Section 3 analyzes the CCF of signals sampled by two important types of sensor kernels: Gaussian and box. Section 4 proposes and justifies the use of the Gaussian function as a parametric model to fit the CCF. In Section 5, this new Gaussian CCF model is applied to time delay estimation, and compared with the existing method. Section 6 reports the simulation results to verify the superior performance of the proposed method. Section 7 concludes the paper.

2. Preliminaries

Consider a continuous information source $s(t)$, which is observed by two sensors with a relative time delay Δ. The discrete sampling procedure is illustrated by Fig. 1. The original signal $s(t)$ and its shift $s(t-\Delta)$ pass through sensor kernel filters $g_1(-t)$ and $g_2(-t)$ respectively to get two smoothed signals:

$$s_1(t) = s(t) * g_1(-t), \qquad s_2(t-\Delta) = s(t-\Delta) * g_2(-t), \tag{2.1}$$

where "$*$" is the convolution operator. Kernels $g_1(t)$ and $g_2(t)$ depend on the physical characteristics of the two sensors. $s_1(t)$ and $s_2(t-\Delta)$ are sampled by two Dirac sequences with period T:

$$x_1(k) = s_1(kT), \qquad x_2(k) = s_2(kT-\Delta). \tag{2.2}$$

Finally the discrete measurements

$$y_1(k) = x_1(k) + \upsilon_1(k), \qquad y_2(k) = x_2(k) + \upsilon_2(k) \tag{2.3}$$

are obtained, where $\upsilon_i(k)$, $i = 1, 2$, are zero-mean observation noises. Here we assume that noises υ_1 and υ_2 are mutually uncorrelated and also uncorrelated with x_1 and x_2.

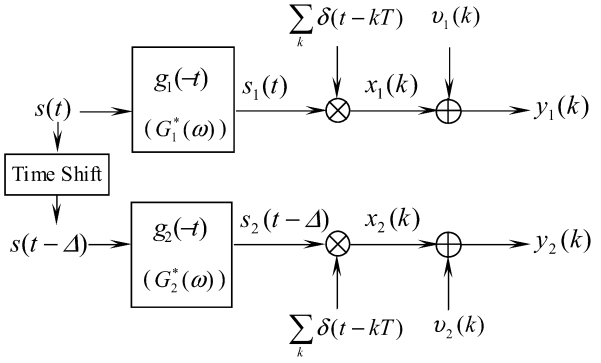

Fig. 1. The sampling process of digital signals $y_1(k)$ and $y_2(k)$.

Assume that $s(t)$ is a stationary process, then its autocorrelation function (ACF) is

$$R_s(\tau) = R_s(-\tau) = E\big\{s(t)s(t+\tau)\big\}. \tag{2.4}$$

The CCF of signals $s_1(t)$ and $s_2(t)$ is given by [16]:

$$R_{12}(\tau) = E\big\{s_1(t)s_2(t+\tau)\big\} = R_s(\tau) * g_1(-\tau) * g_2(\tau). \tag{2.5}$$

In practice, only the observations of $s_1(t)$ and $s_2(t)$, discrete signals $y_1(k)$ and $y_2(k)$, are available. With $y_1(k)$ and $y_2(k)$, which are noisy and sample length limited, we can compute some approximate values of $R_{12}(\tau)$. Since υ_1 and υ_2 are uncorrelated, there is

$$\Re_{12}(n) = \frac{1}{N}\sum_{k=1}^{N} y_1(k)y_2(k+n) \approx E\big\{s_1(t)s_2(t+nT-\Delta)\big\} = R_{12}(nT-\Delta), \tag{2.6}$$

where N is the length of samples used in calculation. $\Re_{12}(n)$ is an approximation of the Dirac sampled value of continuous function $R_{12}(\tau)$ at time $nT-\Delta$. The accuracy of $\Re_{12}(n)$ is affected by the level of measurement noises υ_1 and υ_2 and the sample length N.

The ACF $R_s(\tau)$ peaks at $\tau = 0$. If $g_1(t)$ and $g_2(t)$ are approximately viewed as Dirac functions, then $R_{12}(\tau) = R_s(\tau)$. A widely used method to estimate Δ is to find the peak position of the CCF function approximated by samples $\Re_{12}(n)$. Suppose that $\Re_{12}(n)$ takes on its maximum value at position n_0. If Δ is an integer multiple of sampling period T, then we simply have $\Delta = n_0T$. However, estimating Δ becomes non-trivial, if Δ is a fractional multiple of T and an arbitrary precision of Δ is desired. The current technique is to fit a parabola function with points $\Re_{12}(n_0-1)$, $\Re_{12}(n_0)$ and $\Re_{12}(n_0+1)$, and estimate Δ by the peak position of the fitted parabola [9–11]. This practice is justified if one can show that the parabola is a good approximation of $R_{12}(\tau)$ in the neighborhood of its peak.

The time delay estimation technique of finding the maximum position of CCF is simple, efficient, and can potentially estimate Δ to good precision. But two problems remain open: what is the exact expression of the cross correlation $R_{12}(\tau)$ given some prior knowledge of the auto-correlation $R_s(\tau)$ and sensor kernels, and what is the best model to be used to fit $R_{12}(\tau)$ by the available observations $\Re_{12}(n)$ given a constraint on the model complexity? These are the issues to be addressed in the next sections.

3. Analysis of cross correlation functions

We consider the class of processes of exponential ACF:

$$R_s(\tau) = \alpha \cdot \exp\big(-\beta|\tau|\big), \tag{3.1}$$

where parameters α and β are real numbers. This class of processes can model many natural information sources such as the Gaussian Markov processes. Doob [17] showed that the ACF of any random process which is both Gaussian and Markov can be modeled as an exponential function.

Given ACF $R_s(\tau)$, the form of CCF $R_{12}(\tau)$ depends on the sensor kernels $g_1(t)$ and $g_2(t)$. Ideally, $g_1(t)$ and $g_2(t)$ should be the Dirac functions so that $g_1(t)$ and $g_2(t)$ are full-pass filters. Dirac has the shortest support to get the highest time resolution. Due to the physical limitation of sensors, however, in real systems $g_1(t)$ and $g_2(t)$ are smooth low-pass filters. In many applications, the sensor kernels are approximated by Gaussian functions or the box functions. Next we analyze $R_{12}(\tau)$ in three important cases respectively: both of the kernels are Gaussian; both of the kernels are box functions; one kernel is Gaussian function and the other is box function.

3.1. Two Gaussian kernels

Suppose that kernel $g_i(t)$ is a Gaussian function centered at $t = 0$ with standard deviation v_i, i.e.,

$$g_i(t) = \frac{1}{\sqrt{2\pi}\,v_i}\exp\left(-\frac{t^2}{2v_i^2}\right). \tag{3.2}$$

Without loss of generality, we let the sampling period $T = 1$. We assume that $g_i(t)$ is nearly zero outside $[-T/2, T/2]$. (But the following development is independent of this condition.) To ensure this, we let standard deviation $v_i \leqslant 1/4$. Apparently, when $v_i \to 0$, $g_i(t)$ will approach to a Dirac function.

Since both kernels $g_1(t)$ and $g_2(t)$ are Gaussian, their convolution is also Gaussian. Let

$$G(t) = g_1(-t) * g_2(t) = \frac{1}{\sqrt{2\pi(\nu_1^2+\nu_2^2)}} \exp\left(-\frac{t^2}{2(\nu_1^2+\nu_2^2)}\right) = \frac{1}{\sqrt{2\pi}\nu} \exp\left(-\frac{t^2}{2\nu^2}\right), \tag{3.3}$$

where $\nu = \sqrt{\nu_1^2+\nu_2^2}$ is the standard deviation of $G(t)$. For all $\nu_1, \nu_2 \leqslant 1/4$, we have $\nu \leqslant \sqrt{2}/4$. From (2.5) and (3.1), the CCF $R_{12}(\tau)$ is

$$R_{12}(\tau) = R_s(\tau) * G(\tau) = \frac{\alpha}{\sqrt{2\pi}\nu}\left(\int_0^\infty \exp\left(-\beta t - \frac{(\tau+t)^2}{2\nu^2}\right) dt + \int_0^\infty \exp\left(-\beta t - \frac{(\tau-t)^2}{2\nu^2}\right) dt\right). \tag{3.4}$$

The first item of (3.4) is

$$\int_0^\infty \exp\left(-\beta t - \frac{(\tau+t)^2}{2\nu^2}\right) dt = \sqrt{\pi/2}\cdot\nu\cdot\exp\left(\frac{\nu^2\beta^2+2\tau\beta}{2}\right)\operatorname{erfc}\left(\frac{\nu^2\beta+\tau}{\sqrt{2}\nu}\right),$$

where $\operatorname{erfc}(x) = \frac{2}{\sqrt{\pi}}\int_x^\infty \exp(-t^2)\,dt$ is the complementary error function. Similarly, we can derive the second item of (3.4) to be

$$\int_0^\infty \exp\left(-\beta t - \frac{(\tau-t)^2}{2\nu^2}\right) dt = \sqrt{\pi/2}\cdot\nu\cdot\exp\left(\frac{\nu^2\beta^2-2\tau\beta}{2}\right)\operatorname{erfc}\left(\frac{\nu^2\beta-\tau}{\sqrt{2}\nu}\right).$$

Let

$$f_l(\tau) = \exp(\tau\beta)\operatorname{erfc}\left(\frac{\nu^2\beta+\tau}{\sqrt{2}\nu}\right) \quad \text{and} \quad f_r(\tau) = \exp(-\tau\beta)\operatorname{erfc}\left(\frac{\nu^2\beta-\tau}{\sqrt{2}\nu}\right) \tag{3.5}$$

and

$$f(\tau) = f_l(\tau) + f_r(\tau). \tag{3.6}$$

Then $R_{12}(\tau)$ can be re-written as

$$R_{12}(\tau) = C\cdot f(\tau) \tag{3.7}$$

where $C = \alpha\cdot\exp(\nu^2\beta^2/2)/2$ is a constant independent of τ. Since the shape of $R_{12}(\tau)$ is determined by $f(\tau)$, we turn to examine $f(\tau)$.

In Fig. 2, we plot the curves of $f_l(\tau)$, $f_r(\tau)$ and $f(\tau)$ by setting $\beta = 1$ and $\nu = \sqrt{2}/4$. Since $f(\tau)$ is an even function, it suffices to discuss the case when $\tau \geqslant 0$. Note that the decreasing speed of $\operatorname{erfc}(\frac{\nu^2\beta+\tau}{\sqrt{2}\nu})$ is faster than the increasing speed of $\exp(\tau\beta)$ along the positive abscissa. Therefore, when τ is greater than some positive number, $f_l(\tau) \to 0$ and $\operatorname{erfc}(\frac{\nu^2\beta-\tau}{\sqrt{2}\nu}) \to 2$ and thus

$$f(\tau) \approx f_r(\tau) = \exp(-\tau\beta)\operatorname{erfc}\left(\frac{\nu^2\beta-\tau}{\sqrt{2}\nu}\right) \to 2\exp(-\tau\beta).$$

From Fig. 2 (where $\beta = 1$ and $\nu = \sqrt{2}/4$) we can clearly see this. That is to say, when $|\tau|$ is large, $f(\tau)$ and in turn $R_{12}(\tau)$ can be approximately modeled by an exponential function.

However, in time delay estimation by locating the peak of $R_{12}(\tau)$ we are more interested in the behavior of $R_{12}(\tau)$ in the neighborhood of its peak. The shapes of $f(\tau)$ as well as $R_{12}(\tau)$ depend on two parameters, β, the decaying parameter of $R_s(\tau)$, and ν, the standard deviation of $G(t)$. Fig. 3(a) plots the curves of $f(\tau)$ for $\beta = 1$ in conjunction with varying $\nu = 0.15, 0.2, 0.25, 0.3, 0.35$, whereas Fig. 3(b) shows the curves of $f(\tau)$ for $\nu = 0.25$ and in conjunction with varying $\beta = 0.5, 1, 2, 4, 8$. Referring to the figures, given β, $f(\tau)$ is determined by ν. When ν decreases, Gaussian function $G(x)$ shapes more like a Dirac function, hence $R_{12}(\tau)$ approaches to $R_s(\tau)$ because of the convolution operation $R_{12}(\tau) = R_s(\tau) * G(\tau)$. Similarly, when ν is fixed and β increases, $R_s(\tau)$ approaches to a Dirac function and then the shape of $R_{12}(\tau)$ approaches to the Gaussian function $G(x)$.

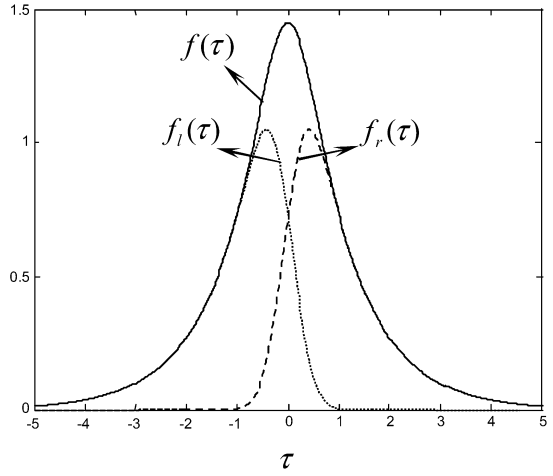

Fig. 2. The curves of $f(\tau)$ (solid), $f_r(\tau)$ (dashed) and $f_l(\tau)$ (dotted) by setting $\beta = 1$ and $\nu = \sqrt{2}/4$.

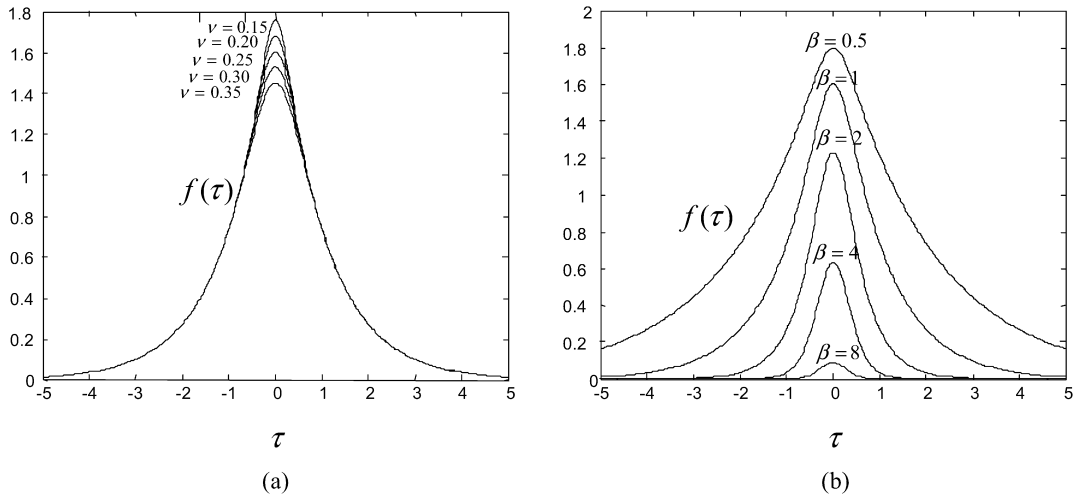

Fig. 3. (a) The curves of $f(\tau)$ by setting $\beta = 1$ and $\nu = 0.15, 0.2, 0.25, 0.3, 0.35$, respectively. (b) The curves of $f(\tau)$ by setting $\nu = 0.25$ and $\beta = 0.5, 1, 2, 4, 8$, respectively.

3.2. Two box kernels

When the sensor kernels are box functions, i.e. kernels $g_i(t), i = 1, 2$, are constant in $[-T/2, T/2]$, the sensors sample the observed process as an integrator in each sampling period. As in the previous subsection, we normalize the sampling period to be $T = 1$ and write $g_i(t)$ as

$$g_i(t) = \begin{cases} 1, & -1/2 \leqslant t \leqslant 1/2, \\ 0, & |t| > 1/2. \end{cases} \tag{3.8}$$

The convolution of box kernels $g_1(t)$ and $g_2(t)$ is

$$G(t) = g_1(-t) * g_2(t) = \begin{cases} 1 + t, & -1 \leqslant t \leqslant 0, \\ 1 - t, & 0 \leqslant t \leqslant 1, \\ 0, & |t| > 1. \end{cases} \tag{3.9}$$

Since both $G(t)$ and $R_s(\tau)$ are even functions, the CCF $R_{12}(\tau) = R_s(\tau) * G(\tau)$ is also an even function, hence we only consider the case for $\tau \geqslant 0$.

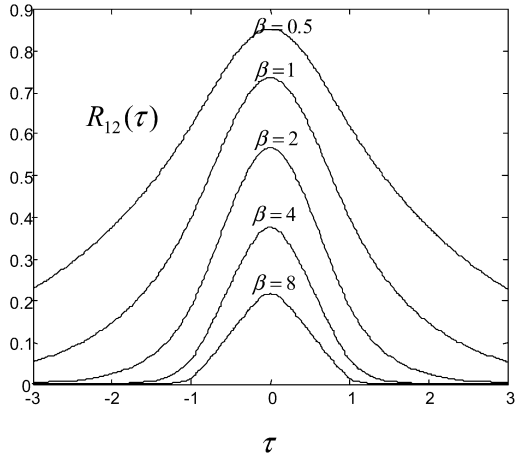

Fig. 4. The curves of $R_{12}(\tau)$ by setting $\alpha = 1$ and $\beta = 0.5, 1, 2, 4, 8$, respectively.

When $0 \leqslant \tau \leqslant 1$, after some tedious computations, we have

$$R_{12}(\tau) = \alpha\left(2\frac{1-\tau}{\beta} + \frac{1}{\beta^2}\exp(-\beta+\beta\tau) + \frac{1}{\beta^2}\big(\exp(-\beta)-2\big)\exp(-\beta\tau)\right). \tag{3.10}$$

When $\tau > 1$, we have

$$R_{12}(\tau) = \frac{\alpha}{\beta^2}\big(\exp(\beta)+\exp(-\beta)-2\big)\exp(-\beta\tau), \quad \tau > 1. \tag{3.11}$$

It can be seen that when $|\tau| > 1$, $R_{12}(\tau)$ is an exponential function of τ, and when $|\tau| \leqslant 1$, $R_{12}(\tau)$ is a linear combination of exponential terms $\exp(-\beta\tau)$ and $\exp(\beta\tau)$ and linear term τ.

The shape of $R_{12}(\tau)$ is controlled by parameter β. (Parameter α only affects the magnitude scale of $R_{12}(\tau)$.) With the increasing of β, $R_s(\tau)$ approaches to a Dirac function so that CCF $R_{12}(\tau)$ approaches to $G(t)$ defined in (3.9), which is actually the first order spline function. In Fig. 4 we show the curves of $R_{12}(\tau)$ in interval $[-3, 3]$ for $\beta = 0.5, 1, 2, 4, 8$. (The scale parameter α is set to 1.)

3.3. One Gaussian and one box kernels

Suppose sensor kernel $g_1(t)$ is Gaussian function as defined in (3.2) and the other sensor kernel $g_2(t)$ is box function as defined in (3.8), then the convolution of $g_2(t)$ and $g_1(t)$ is

$$G(t) = g_2(-t) * g_1(t) = \frac{1}{2}\operatorname{erf}\left(\frac{t+1/2}{\sqrt{2}\nu_1}\right) - \frac{1}{2}\operatorname{erf}\left(\frac{t-1/2}{\sqrt{2}\nu_1}\right), \tag{3.12}$$

where $\operatorname{erf}(x) = \frac{2}{\sqrt{\pi}}\int_0^x \exp(-t^2)\,dt$ is the error function. Apparently $G(t)$ is an even function and takes its maximum at $t = 0$. The CCF $R_{12}(\tau)$ is computed to be

$$R_{12}(\tau) = R_s(\tau) * G(\tau) = \alpha\int_0^\infty \exp(-\beta t)\cdot\big(G(\tau+t)+G(\tau-t)\big)\,dt. \tag{3.13}$$

Since error function $\operatorname{erf}(x)$ is not integrable, we cannot express $R_{12}(\tau)$ in terms of a finite number of elementary functions.

The shape of CCF $R_{12}(\tau)$ is controlled by two parameters: ν_1, the deviation of Gaussian kernel $g_1(t)$, and β, the decay speed of ACF $R_s(\tau)$. Let constant $\alpha = 1$, Fig. 5(a) plots $R_{12}(\tau)$ for $\beta = 1$ and $\nu_1 = 0, 0.15, 0.25$, respectively. We see that $R_{12}(\tau)$ does not vary much on ν_1 in the interval $\nu_1 \in [0, 0.25]$. Fig. 5(b) plots $R_{12}(\tau)$ for $\beta = 0.5, 1, 2, 4, 8$, respectively by setting $\nu_1 = 0.25$. When β increases, $R_s(\tau)$ approaches to a Dirac function, so that the shape of $R_{12}(\tau)$ is close to that of $G(\tau)$.

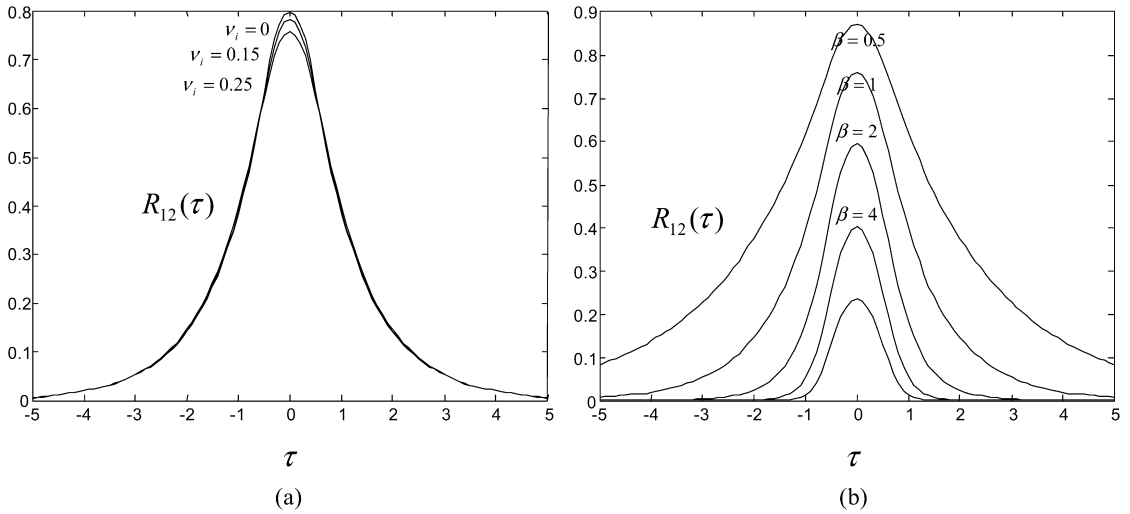

Fig. 5. (a) The curves of $R_{12}(\tau)$ by setting $\beta = 1$ and $\nu_1 = 0, 0.15, 0.25$, respectively. (b) The curves of $R_{12}(\tau)$ by setting $\nu_1 = 0.25$ and $\beta = 0.5, 1, 2, 4, 8$, respectively.

4. Parametric models of cross correlation function

Unfortunately, the precise CCF $R_{12}(\tau)$ does not have a simple closed form, as revealed by the analyses in the previous section. But we have shown that $R_{12}(\tau)$ is a smooth even function. Furthermore, an inspection of Figs. 3–5 indicates that $R_{12}(\tau)$ exhibits a quadratic-like behavior near the peak for Gaussian and/or box sensor kernels. This explains the past success of fitting three points $\Re_{12}(n_0-1)$, $\Re_{12}(n_0)$ and $\Re_{12}(n_0+1)$ to a parabola as an approximation of $R_{12}(\tau)$ near the peak of $R_{12}(\tau)$ [9–11], where $\Re_{12}(n_0)$ is the maximum point of the computed CCF samples (referring to (2.6)).

Denote the parabola function as $f_p(x) = ax^2 + bx + c$. Parameters a, b and c are determined by

$$\begin{bmatrix} a \\ b \\ c \end{bmatrix} = \begin{bmatrix} 1 & -1 & 1 \\ 0 & 0 & 1 \\ 1 & 1 & 1 \end{bmatrix}^{-1} \begin{bmatrix} \Re_{12}(n_0-1) \\ \Re_{12}(n_0) \\ \Re_{12}(n_0+1) \end{bmatrix}. \tag{4.1}$$

The next natural question is if there exists a better model of $R_{12}(\tau)$ than parabola function given the same number of model parameters. A causal revisit of Figs. 3–5 suggests that Gaussian function

$$f_g(x) = a \cdot \exp\bigl(-b(x-c)^2\bigr) \tag{4.2}$$

is a good candidate model of $R_{12}(\tau)$ in the interval around its peak position. The three parameters are determined as follows. Let $\Re_{12}(n_0-1) = f_g(-1)$, $\Re_{12}(n_0) = f_g(0)$ and $\Re_{12}(n_0+1) = f_g(1)$, we have

$$\begin{cases} \ln \Re_{12}(n_0-1) = \ln a - b(1+c)^2, \\ \ln \Re_{12}(n_0) = \ln a - bc^2, \\ \ln \Re_{12}(n_0+1) = \ln a - b(1-c)^2. \end{cases} \tag{4.3}$$

Solving the above equation set, we get

$$a = \exp\left\{ \ln \Re_{12}(n_0) + \frac{(\ln \Re_{12}(n_0+1) - \ln \Re_{12}(n_0-1))^2}{16 \ln \Re_{12}(n_0) - 8 \ln \Re_{12}(n_0-1) - 8 \ln \Re_{12}(n_0+1)} \right\}, \tag{4.4a}$$

$$b = \frac{2 \ln \Re_{12}(n_0) - \ln \Re_{12}(n_0-1) - \ln \Re_{12}(n_0+1)}{2}, \tag{4.4b}$$

$$c = \frac{\ln \Re_{12}(n_0+1) - \ln \Re_{12}(n_0-1)}{4 \ln \Re_{12}(n_0) - 2 \ln \Re_{12}(n_0-1) - 2 \ln \Re_{12}(n_0+1)}. \tag{4.4c}$$

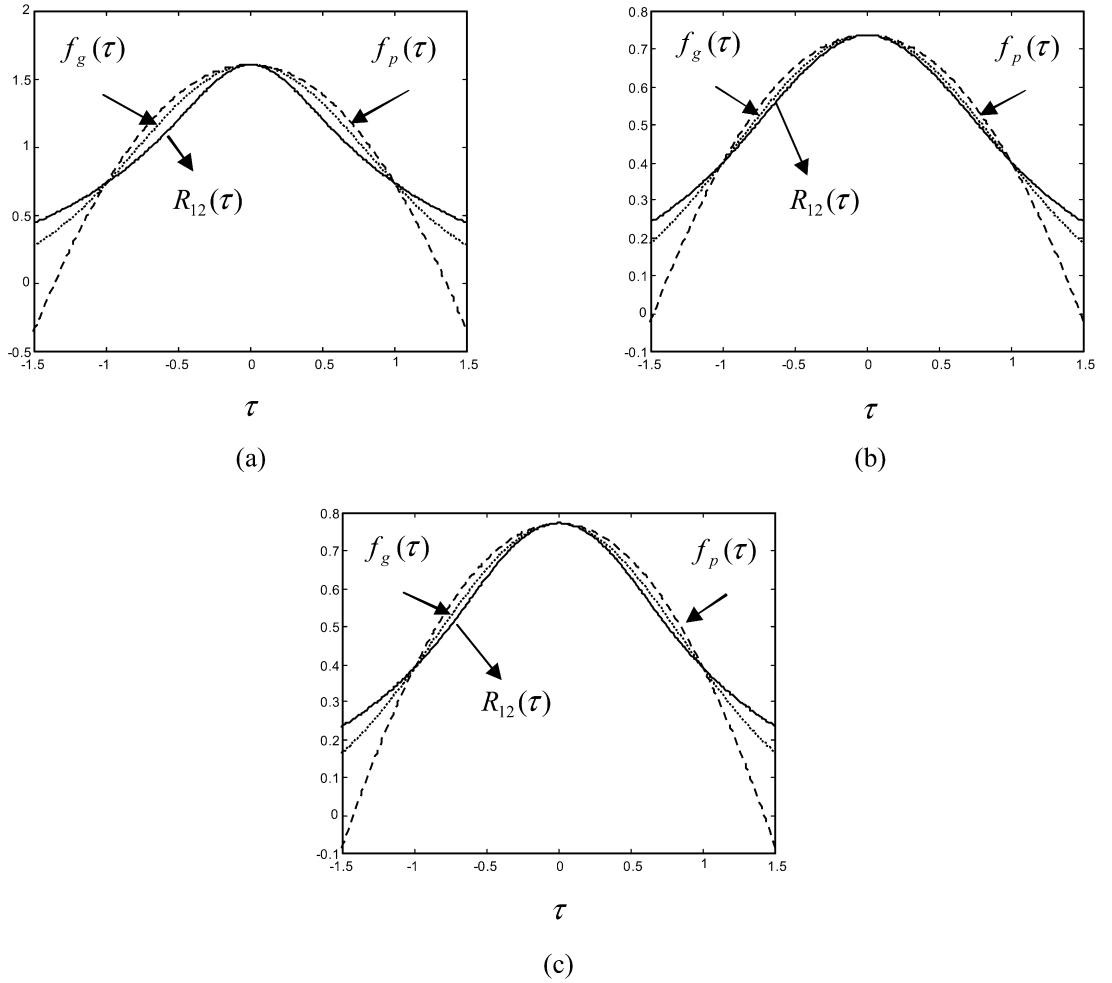

Fig. 6. The true CCF $R_{12}(\tau)$ (solid) compared with the fitted CCFs by parabola model (dashed) and Gaussian model (dotted) for the case that (a) both sensor kernels are Gaussian ($\beta = 1$ and $\nu = 0.25$); (b) both sensor kernels are box ($\beta = 1$); (c) one sensor kernel is Gaussian and the other is box ($\beta = 1$ and $\nu_1 = 0.2$).

Let $\Re_{12}(n_0) = R_{12}(0)$, $\Re_{12}(n_0-1) = R_{12}(-1)$ and $\Re_{12}(n_0+1) = R_{12}(1)$, in Fig. 6 we plot true curves of $R_{12}(\tau)$ in the neighborhood of its peak together with the fitted curves of $R_{12}(\tau)$ by the parabola and Gaussian models. Fig. 6(a) is for the case that both sensor kernels are Gaussian, $\beta = 1$ and $\nu = 0.25$. Fig. 6(b) is for the case that both sensor kernels are box and $\beta = 1$. Fig. 6(c) is for the case that one sensor kernel is Gaussian and the other is box, $\beta = 1$ and $\nu_1 = 0.2$. We see that the curves fitted by the Gaussian model are closer to the true CCF functions than those fitted by the parabola model.

5. Time delay estimation

In this section we apply the above Gaussian model of $R_{12}(\tau)$ to time delay estimation, and evaluate its performance against the parabola model. Suppose that $\Re_{12}(n)$ are the true discrete samples of the continuous function $R_{12}(\tau)$, i.e., $\Re_{12}(n) = R_{12}(nT - \Delta)$. The task of time delay estimation is to determine Δ from the model fitted by points $\Re_{12}(n_0 - 1)$, $\Re_{12}(n_0)$ and $\Re_{12}(n_0 + 1)$.

If Δ is an integer multiple of sampling period T, then $R_{12}(n_0T - \Delta)$ is the maximum value of $R_{12}(\tau)$, hence $n_0T - \Delta = 0$ or $\Delta = n_0T$. However, in practice Δ has an arbitrary real value. The fractional part of Δ can be written as $\Delta_\varepsilon = \Delta - n_0T$. With the parabola model, the fractional part Δ_ε is estimated as $\hat{\Delta}_p = -\frac{b}{2a}T$, where a and b are determined by (4.1). For Gaussian model, the fractional part Δ_ε is estimated as $\hat{\Delta}_g = cT$,

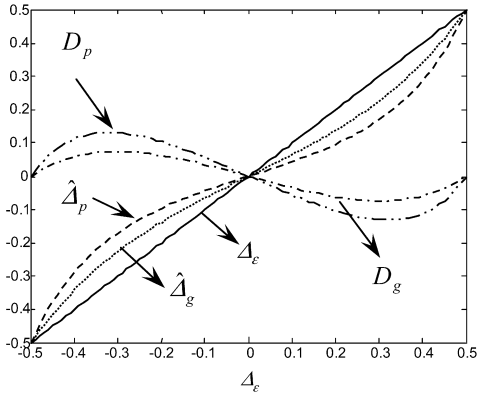

Fig. 7. The curves of $\hat{\Delta}_p$ (dashed), $\hat{\Delta}_g$ (dotted), D_p (long-dashdotted) and D_g (short-dashdotted) vs. Δ_ε (the solid diagonal line) for $\beta = 1$ and $\nu = 0.25$.

where c is determined by (4.4c). Denote by D_p and D_g the estimation errors of the two different fitting models:

$$D_p = \hat{\Delta}_p - \Delta_\varepsilon \quad \text{and} \quad D_g = \hat{\Delta}_g - \Delta_\varepsilon. \tag{5.1}$$

Next we compare the estimation errors D_p and D_g via numerical computations.

5.1. Results for Gaussian sensor kernels

If sensor kernels $g_1(t)$ and $g_2(t)$ are Gaussian, the CCF $R_{12}(\tau)$ is determined by (3.5)–(3.7). The shape of $R_{12}(\tau)$ is controlled by parameters β and ν. Normalize the sampling period $T = 1$, so that the fractional part of Δ is $\Delta_\varepsilon \in [-0.5, 0.5]$. We increase Δ_ε from -0.5 to 0.5, and sample $\Re_{12}(n_0 - 1)$, $\Re_{12}(n_0)$ and $\Re_{12}(n_0 + 1)$ from $R_{12}(\tau)$ to compute the parabola and Gaussian estimates of Δ_ε, i.e. $\hat{\Delta}_p$ and $\hat{\Delta}_g$, as well as their estimation errors D_p and D_g. In Fig. 7, we plot the curves of $\hat{\Delta}_p$, $\hat{\Delta}_g$, D_p and D_g for $\beta = 1$ and $\nu = 0.25$. We see that the magnitude of estimation error D_p is always higher than that of D_g. Comparisons for other values of β and ν draw the same conclusion. We define the mean absolute errors (MAS) of $\hat{\Delta}_p$ and $\hat{\Delta}_g$ as

$$E_p = \int_{-0.5}^{0.5} \left|D_p(\Delta_\varepsilon)\right| d\Delta_\varepsilon \quad \text{and} \quad E_g = \int_{-0.5}^{0.5} \left|D_g(\Delta_\varepsilon)\right| d\Delta_\varepsilon. \tag{5.2}$$

Fig. 8 plots E_p and E_g as two-dimensional functions over $\nu \in [0.05, 0.35]$ and $\beta \in (0, 10]$. Clearly, the estimation error E_p is higher than E_g in the entire range of (ν, β). Both E_p and E_g decrease in ν. However, with the increasing of β, E_p increases rapidly but E_g decreases. These observations can be explained as follows. First, a smaller ν makes $G(t)$ (referring to (3.3)) sharper and closer to a Dirac function, so that $R_{12}(\tau)$ shapes more like the ACF $R_s(\tau)$, which is an exponential function, due to the convolution operation $R_{12}(\tau) = R_s(\tau) * G(\tau)$. Therefore the fitting error between $R_{12}(\tau)$ and parabola $f_p(x)$ or Gaussian function $f_g(x)$ increases in ν, so does the MAS E_p or E_g. Second, a larger β drives $R_s(\tau)$ closer to a Dirac function, so that $R_{12}(\tau)$ approaches to $G(t)$, which is a Gaussian function, due to the convolution operation, then the fitting error between $R_{12}(\tau)$ and Gaussian function $f_g(x)$ decreases in β, whereas the fitting error between $R_{12}(\tau)$ and parabola $f_p(x)$ increases. This is the reason why MAS E_p and E_g have opposite trends in β.

Finally, we point out that, as being evident in Figs. 8(a) and (b), the Gaussian approximation of CCF $R_{12}(\tau)$ is more robust than the parabola approximation in time delay estimation, for the former consistently achieves smaller estimation error than the latter over different Gaussian kernels.

5.2. Results for box sensor kernels

When both kernels $g_1(t)$ and $g_2(t)$ are box functions, the CCF $R_{12}(\tau)$ is given by (3.10), (3.11) and its shape is controlled by parameter β only. As in (5.2), we denote by E_p and E_g the MAS of estimates $\hat{\Delta}_p$ and $\hat{\Delta}_g$. Fig. 9

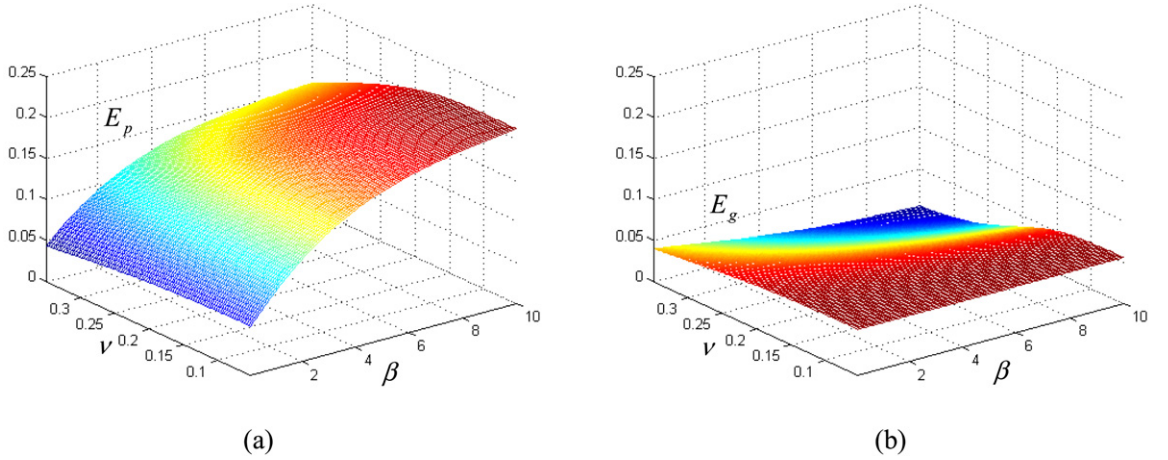

Fig. 8. (a) The E_p surface vs. parameters ν and β. (b) The E_g surface vs. parameters ν and β.

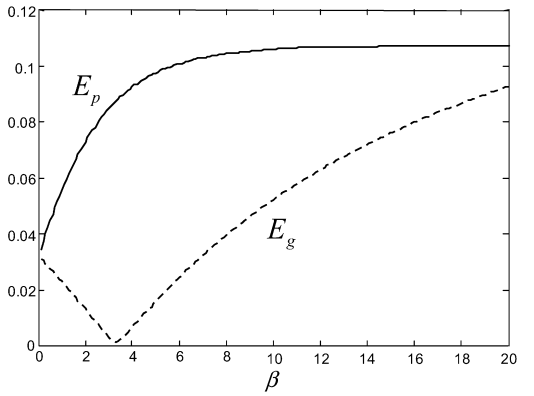

Fig. 9. The curves of E_p (solid) and E_g (dashed) versus parameter β.

plots the curves of E_p and E_g versus parameter β in interval $(0, 20]$. We see that E_p increases in β and it flattens out when $\beta > 10$. In a wide range of β, E_g is much less than E_p, and becomes greater than E_p only when $\beta > 26$. In real applications β is usually small, rarely greater than 10. A large value of β means the considered process is nearly a white process whose ACF is a Dirac pulse. E_g reaches the minimum around $\beta = 3.3$. At this position E_g is very close to zero, and here $R_{12}(\tau)$ can be almost perfectly approximated by a Gaussian function. E_g decreases when $\beta \in (0, 3.3]$, but increases when $\beta \in [3.3, \infty]$. As β gets larger, the ACF $R_s(\tau)$ becomes closer to a Dirac function so that the $R_{12}(\tau)$ approaches to function $G(t)$ in (3.9). Consequently the fitting error between $R_{12}(\tau)$ and the Gaussian function $f_g(x)$, as well as the MAS E_g, increases in β.

5.3. Results for hybrid Gaussian and box sensor kernels

When one sensor kernel $g_1(t)$ is Gaussian while the other kernel $g_2(t)$ is a box function, the CCF $R_{12}(\tau)$ is determined by (3.13) and its shape controlled by parameters ν_1 and β. In Fig. 10 we plot E_p and E_g over $\nu_1 \in [0.01, 0.25]$ and $\beta \in (0, 10]$. Clearly, E_p lies above E_g for all (ν_1, β), and is far more sensitive than E_g to parameters ν_1 and β. Although the time delay estimation of Gaussian model is more robust than the parabola model, the behavior of E_g is more complex than E_p in the (ν_1, β) plane. Interestingly, Fig. 10(b) shows that on the surface of E_g there is a curve along which E_g is nearly zero and reaches its minimum point with respect to ν_1 or β.

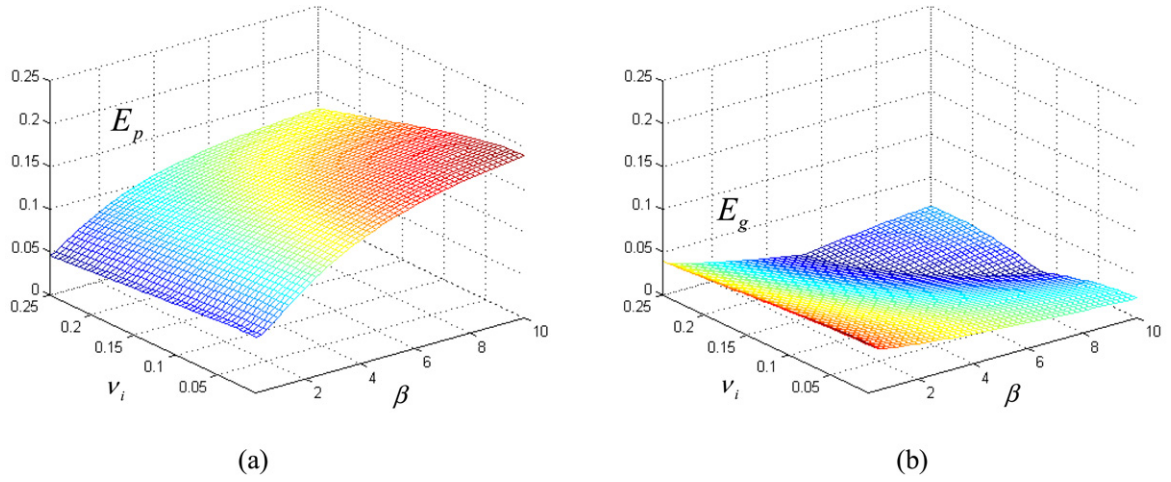

Fig. 10. (a) The mesh figure of E_p in the plane determined by parameters ν_1 and β. (b) The mesh figure of E_g in the plane determined by parameters ν_1 and β.

6. Simulation results

The above analytical results were obtained under the assumption that $\Re_{12}(n_0-1)$, $\Re_{12}(n_0)$ and $\Re_{12}(n_0+1)$ are ideally sampled from $R_{12}(\tau)$, i.e., $\Re_{12}(n) = R_{12}(nT-\Delta)$. In practice, $\Re_{12}(n)$ is a noisy observation and hence only an approximation of the true value of $R_{12}(nT-\Delta)$. In this section, we simulate the noisy data $y_1(k)$ and $y_2(k)$ and evaluate the performance of the proposed time delay estimation method in comparison with the parabola model.

First the continuous process $s(t)$ is simulated by a first order Gaussian Markov process, whose ACF is an exponential function $R_s(\tau) = R_s(0)\cdot a^{\tau}$ with $0<a<1$. Then smoothed signals $s_i(t)$, $i=1,2$, are obtained by passing $s(t)$ and its shift $s(t-\Delta)$ through the sensor kernels $g_i(t)$: $s_1(t) = s(t) * g_1(-t)$ and $s_2(t) = s(t-\Delta) * g_2(-t)$. Let the sampling period $T=1$. The discrete signals $x_i(k)$ are obtained by directly sampling $s_i(t)$: $x_1(k) = s_1(k)$ and $x_2(k) = s_2(k-\Delta)$. The corresponding measurement $y_i(k)$ is made to be $y_i(k) = x_i(k) + \upsilon_i(k)$, where υ_i is a sequence of zero mean Gaussian white noises which is uncorrelated with x_i. Noise sequences υ_1 and υ_2 are also uncorrelated. Denote by σ_1 and σ_2 the standard deviations of υ_1 and υ_2. The signal to noise ratio (SNR) of y_1 or y_2 is computed as

$$\mathrm{SNR} = 10\cdot\log_{10}\bigl(\mathrm{Var}(x_i)/\sigma_i^2\bigr), \tag{6.1}$$

where $\mathrm{Var}(x_i)$ is the variance of x_i. The approximated samples of CCF $R_{12}(\tau)$ are computed by

$$\Re_{12}(n) = \frac{1}{N}\sum_{k=1}^{N} y_1(k)y_2(k+n), \tag{6.2}$$

where N is the number of used samples to compute $\Re_{12}(n)$.

In the following experiments, we set the parameter $a=0.95$ in generating $s(t)$ and let the relative time delay Δ vary from -0.5 to 0.45 with a step length 0.05. For each Δ, we compute the time delay estimation errors $D_p(\Delta)$ and $D_g(\Delta)$ by the method described in Section 5 and compute the MAS by

$$E_p = \frac{1}{20}\sum_{\Delta=-0.5}^{0.45}\bigl|D_p(\Delta)\bigr| \quad\text{and}\quad E_g = \frac{1}{20}\sum_{\Delta=-0.5}^{0.45}\bigl|D_g(\Delta)\bigr|. \tag{6.3}$$

We first conduct experiments to observe the effect of parameter N on E_p and E_g. Fixing the SNR of y_1 and y_2 to be 20 dB, we exponentially increase N from 2^4 to 2^9. For each value of N we performed 1000 times the simulation and computed the average values of E_p and E_g. Fig. 11(a) shows the curves of E_p and E_g versus $\log_2 N$ for the case that both sensor kernels are Gaussian. (The standard deviations of the Gaussian kernels are $\nu_1=\nu_2=0.2$.) Fig. 11(b)

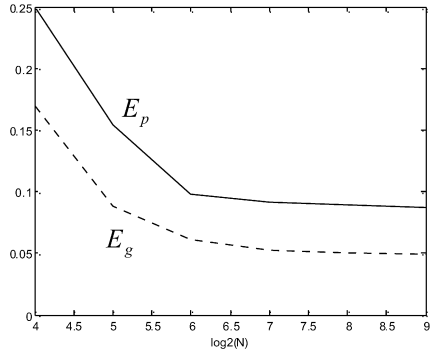

(a)

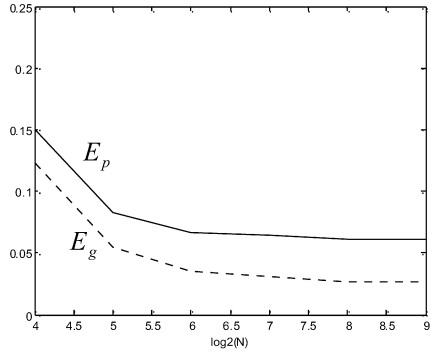

(b)

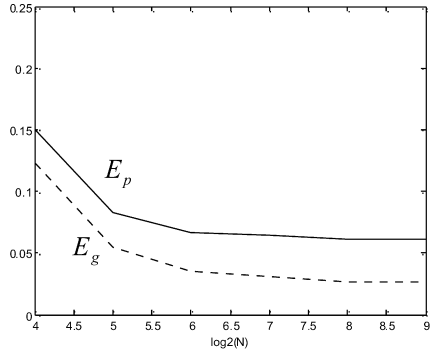

(c)

Fig. 11. The curves of E_p (solid) and E_g (dashed) vs. sample window size $\log_2 N$ for (a) two Gaussian kernels; (b) two box kernels; (c) one Gaussian kernel and one box kernel.

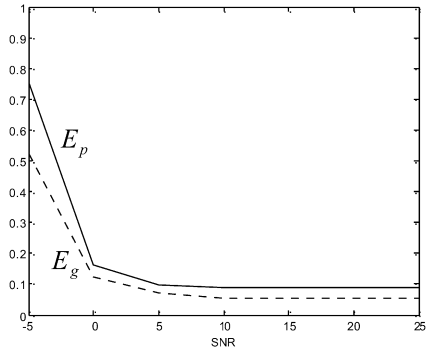

(a)

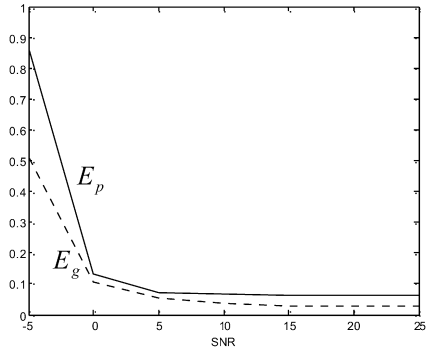

(b)

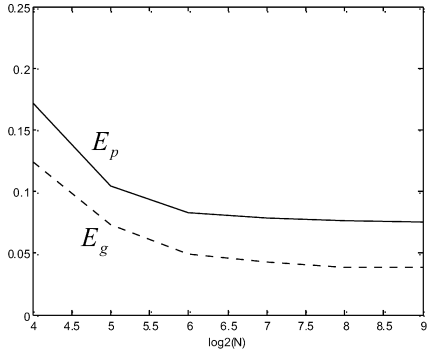

(c)

Fig. 12. The curves of E_p (solid) and E_g (dashed) vs. SNR for (a) two Gaussian kernels; (b) two box kernels; (c) one Gaussian kernel and one box kernel.

is the result for the case that both kernels are box functions. Fig. 11(c) is the result for case that one sensor kernel is Gaussian ($\nu_1 = 0.2$) and the other sensor kernel is box. As expected, E_p and E_g decrease with the increasing of the sample window size N, and flatten out near $N = 2^6$. For any value of N, E_g is always less than E_p.

Next we compute E_p and E_g for varying SNRs of y_1 and y_2. We fix the sample length N to be 256, and increase the SNR of y_1 and y_2 from -5 dB to 25 dB. For each SNR level we performed 1000 times the simulation and computed the average values of E_p and E_g. Figs. 12(a)–(c) illustrate the curves of E_p and E_g versus SNR for the three cases of sensor kernels. We see that E_p and E_g decrease with the increasing of SNR. When SNR $\geqslant 6$ dB, E_p and E_g are nearly constants. Over the entire range of SNR, E_g is consistently smaller than E_p. It can be readily observed from the figures that the proposed time delay estimation method based on Gaussian approximation of CCF is more robust than the existing method, and its advantage becomes more significant as noise level increases.

7. Conclusion

The cross correlation function (CCF) of two signals observed by different sensors was studied in this paper. Analytic forms of CCFs were derived and their behaviors were examined for stationary processes whose auto-correlation function is exponential and for two important types of sensor sampling kernels: Gaussian and box. A Gaussian approximation model of CCF was proposed and shown to be more accurate and robust than the current parabola-based model. The proposed model was investigated in the application of time delay estimation. Simulations were conducted to verify the analytical findings. The new method outperforms the existing one, with the improvement being more significant on highly noisy signals.

References

[1] D.L. Hall, J. Llinas, An introduction to multisensor data fusion, Proc. IEEE 85 (1997) 6–23.
[2] M.E. Liggins II, C.-Y. Chong, I. Kadar, M.G. Alford, V. Vannicola, S. Thomopoulos, Distributed fusion architectures and algorithms for target tracking, Proc. IEEE 85 (1997) 95–107.
[3] R.J. Vaccaro, The past, present, and the future of underwater acoustic signal processing, IEEE Signal Process. Mag. 15 (1998) 21–51.
[4] Nabaa, R.H. Bishop, Solution to a multisensor tracking problem with sensor registration errors, IEEE Trans. Aerosp. Electron. Syst. 35 (1999) 354–363.
[5] R.R. Schultz, L. Li Meng, R.L. Stevenson, Subpixel motion estimation for super-resolution image sequence enhancement, J. Visual Commun. Image Represent. 9 (1998) 38–50.
[6] C.H. Knapp, G.C. Carter, The generalized correlation method for estimation of time delay, IEEE Trans. Acoust. Speech Signal Process. 24 (1976) 320–327.
[7] M. Azaria, D. Hertz, Time delay estimation by generalized cross correlation methods, IEEE Trans. Acoust. Speech Signal Process. 32 (1984) 280–285.
[8] G.C. Carter, Coherence and time delay estimation, Proc. IEEE 75 (1987) 236–255.
[9] A. Fertner, A. Sjolund, Comparison of various time delay estimation methods by computer simulation, IEEE Trans. Acoust. Speech Signal Process. 34 (1986) 1329–1330.
[10] R. Moddemeijer, On the determination of the position of extrema of sampled correlators, IEEE Trans. Signal Process. 39 (1990) 216–219.
[11] G. Jacovitti, G. Scarano, Discrete time techniques for time delay estimation, IEEE Trans. Signal Process. 41 (1993) 525–533.
[12] A. Kumar, Y. Bar-Shalom, Time-domain analysis of cross correlation for time delay estimation with an autocorrelated signal, IEEE Trans. Signal Process. 41 (1993) 1664–1668.
[13] Y.T. Chan, H.C. So, P.C. Ching, Approximate maximum likelihood delay estimation via orthogonal wavelet transform, IEEE Trans. Signal Process. 47 (1999) 1193–1198.
[14] H.-H. Chiang, C.L. Nikias, A new method for adaptive time delay estimation for non-Gaussian signals, IEEE Trans. Acoust. Speech Signal Process. 38 (1990) 209–219.
[15] M. Simaan, Frequency domain alignment of discrete time signals, IEEE Trans. Acoust. Speech Signal Process. 32 (1984) 656–659.
[16] A. Papoulis, Probability, Random Variables, and Stochastic Processes, third ed., McGraw–Hill, New York, 1991.
[17] J.L. Doob, Topics in the theory of Markov chains, Trans. Amer. Math. Soc. 52 (1942) 37–64.

Lei Zhang received the B.S. degree in 1995 from Shenyang Institute of Aeronautical Engineering, Shenyang, PR China, the M.S. and Ph.D. degrees in Electrical and Engineering from Northwestern Polytechnical University, Xi'an, PR China, respectively in 1998 and 2001. From 2001 to 2002, he was a research associate in the Department of Computing, The Hong Kong Polytechnic University. From January 2003 to January 2006 he worked as a Postdoctoral Fellow in the Department of Electrical and Computer Engineering, McMaster University, Canada. Since January 2006, he has been an Assistant Professor in the Department of Computing, The Hong Kong Polytechnic University. His research interests include Image and Video Processing, Biometrics, Pattern Recognition, Multisensor Data Fusion and Optimal Estimation Theory, etc. He is a member of IEEE and an associate editor of IEEE Trans. on SMC-C.

Xiaolin Wu Xiaolin Wu got his B.Sc. from Wuhan University, China in 1982, and Ph.D. from University of Calgary, Canada in 1988. He is currently a professor at the Department of Electrical & Computer Engineering, McMaster University, Ontario, Canada, and a research professor of Computer Science, Polytechnic University, Brooklyn, NY, USA, and holds the NSERC-DALSA research chair in Digital Cinema. His research interests include multimedia coding and communications, image processing, signal quantization and compression, and joint source-channel coding. He has published over one hundred research papers and holds two patents in these fields. His awards include 2003 Nokia Visiting Fellowship, 2000 Monsteds Fellowship, and 1998 UWO Distinguished Research Professorship.